



MINISTRY OF TECHNOLOGY

AERONAUTICAL RESEARCH COUNCIL
REPORTS AND MEMORANDA

Stress Concentration Factors for Reinforced Rounded-Square Holes in Sheets

By A. J. Sobey

ROYAL AIR FORCE
BEDFORD.

LONDON: HER MAJESTY'S STATIONERY OFFICE

1968

PRICE 10s. 6d. NET

Stress Concentration Factors for Reinforced Rounded-Square Holes in Sheets

By A. J. SOBEY

*Reports and Memoranda No. 3546**
January, 1967

Summary.

The influence of a uniformly reinforced 'rounded-square' hole on the stress field in an infinite sheet is examined. Stress concentration factors are presented in graphical form for a wide range of corner quadrant radius and reinforcement parameters.

CONTENTS

1. Introduction

2. Analysis

- 2.1. Mapping of hole
- 2.2. Stress potentials
- 2.3. Stress criteria

3. Discussion of Results

Appendix A The effect of a finite bending stiffness of the edge reinforcement on the shear stress under a pressure discontinuity

Appendix B Circular reinforced holes

List of Symbols

References

Illustrations—Figs. 1 to 23

Detachable Abstract Cards

1. Introduction.

The presence of cut-outs in stressed sheets poses considerable problems in design. Even in the simplest configurations, where the hole is unreinforced, little progress was made until the development of the powerful complex variable methods of Muskhelishvili¹. Even so, the analysis of the stresses around a hole of arbitrary shape presents considerable difficulty since it is necessary to find a transformation (or mapping) of the profile of the hole on to a circle. In analysing the simplest geometrical shapes (e.g. ellipses) for which results had previously been recovered using expansions of the Airy stress function in appropriate co-ordinate systems, it is found that the mapping function is a simple 2- or 3-term polynomial. More complicated shapes, particularly those with curvature discontinuities such as slots, require, in practice, very extensive mapping functions if the profile is to be represented to a sufficient accuracy for structural analysis purposes. A procedure for the development of an appropriate mapping function has already been given by the author² which is well suited to modern computing machines; a series of profiles of the slot (and other) types was examined and considerable design information presented².

If the hole is to be reinforced, which is usually essential, the analysis becomes much more difficult. Mansfield⁴ has shown how the hole may be designed so that conditions in the sheet are unchanged by the presence of the hole. Such a hole is said to be 'neutral'. In order to neutralise a hole, it is necessary not only to use a specific shape for the hole, which is determined by loading conditions in regions remote from the hole, but also to use that particular distribution of edge reinforcement which will ensure equilibrium of load and compatibility of strain at the attachment interface. Frequently, in practice, one or other of these specifications has to be waived. For reasons of access the preferred shape of the hole may not be the neutral one: for manufacturing and other reasons, the neutral distribution of edge reinforcement may not be employed.

The weight of the edge reinforcement indicated by neutral hole theory may be as high as 2 or 3 times the weight of sheet removed. The cost in structure weight of keeping the stress level uniformly low may be too great in practice and it may be more profitable to allow the stress to rise by reducing the reinforcement and achieving a lighter system. Mansfield⁵ and Wittrick⁶ have discussed the elliptical hole which is neutral for 2:1 biaxial loading in the sheet and have shown that the use of a constant cross-section reinforcement of appropriate size, leads to a small rise in stress with associated weight economy. Even though it may not be practicable to use the neutral design, neutral hole theory is valuable in indicating the best shape of hole to use, even when the designer has no intention of reinforcing the hole according to neutral hole theory.

The analysis of the stress around a hole of *arbitrary* shape and reinforcement presents a much more complicated problem. Wittrick⁶ has extended the unreinforced hole solution of Muskhelishvili to cover the elastic boundary condition appropriate to the sheet stiffener interface. The stiffener is assumed to be compact and of negligible bending stiffness (a 'chain') as introduced in the neutral hole theory. In practice the stiffness of the stiffener is not likely to influence the stress distribution around the hole markedly except near a curvature discontinuity as discussed later. Wittrick's analysis leads to cumbersome arithmetic even in the most favourable cases with 2- or 3-term mapping functions (as, for example, the elliptic hole which he discussed⁷). Infinite series are required to express the complex stress potentials and only for certain particular configurations indicated by Wittrick does the analysis reduce to the relative simplicity of the unreinforced case. When the mapping function is extensive, the arithmetic becomes unwieldy but such difficulties have to be accepted in analysing reinforced slot type holes.

In this Report Wittrick's theory is applied to a group of rounded-square profiles whose boundaries are composed of quadrants of circles and straight lines. Because of the jump in curvature at the junction of the straight and curved boundary elements, the representation of the profile can only be approximate³ but for the unreinforced hole no practical difficulties arise in approximating to the stress field. For the reinforced hole, however, analysed by the Wittrick theory, the supposition that the reinforcement is of chain type leads to a local distribution of the stress field around a discontinuity in curvature. This perturbation of the stress field arises from the simplification of the stiffener properties: in practice there will be no local concentration of stress at the curvature jump since the stiffener will possess some bending stiffness. However small that stiffness may be, it will ensure continuity of the edge loads induced into the sheet at the interface and the stress field will be free of singularities.

Wittrick⁸ has examined the stress distribution around a class of profiles of the 'rounded-square' type. These have continuous variation of curvature and their affinity to the truly quadrantal profile is discussed in Ref. 3. In this Report, the true quadrantal corner profiles are examined and a comparison with the simpler representation is provided. The variation of stress concentration with geometrical parameters is provided and results are given both for the Mises-Hencky and for the maximum principal stress criteria.

2. Analysis.

The complex-variable methods of Muskhelishvili¹ for the analysis of the 2-dimensional stress system in a sheet perforated by a single hole have been extended by Wittrick⁶ to deal with a reinforced boundary at the hole. The analysis is not repeated here and Wittrick's notation is, in the main, adopted. Stress potentials have to be constructed as expansions in an auxiliary complex-variable ζ which have a known behaviour at infinity, where the influence of the hole is negligible. If the function mapping the hole on to the unit-circle in the ζ -plane is known, the stresses are exactly calculable as polynomials in the unreinforced case. However, if the hole is reinforced, the 'chain' boundary condition cannot be satisfied exactly using finite series for the stress potentials except for a few special cases enumerated by Wittrick⁶. Instead, it has to be satisfied approximately and collocation methods, as proposed by Wittrick, are found to be quite satisfactory.

2.1. Mapping of the Hole.

The significant difference between the investigation reported here and Wittrick's applications^{7,8} is in the nature of the profile of the hole. Wittrick has used 2- and 3-term mapping functions to transform the given profile on to the unit-circle in the ζ -plane. These correspond to the elliptic hole⁷ and the 'rounded-square'⁸ or Wittrick profile³. Both these families of profiles have continuous and smooth variation of curvature in contrast with the profiles analysed here and elsewhere³. To obtain reasonable transformations many terms are required in the mapping function and an adequate simulation of the profile is achieved using 40-term polynomials. The exact profile to which the mapping corresponds can be regarded as a perturbation of the given one, and for light reinforcements, the errors in the stress systems developed will not be significant. To avoid the worst effects of the perturbation, standard smoothing techniques are used⁹.

Difficulties arise when attempts are made to map a profile with abrupt changes in curvature, owing to the Gibbs' phenomenon, but these can be alleviated by replacing the neighbourhood of the curvature jump by a 'ramp' of rapidly changing curvature. This can be done by modifying the mapping coefficients using the Féjer or Sigma corrections⁹. The Sigma correction is used in this Report and the coefficients C_n of the mapping function

$$z = \sum_{-1}^N C_n \zeta^{-n}$$

are modified to

$$C_n \sin \alpha/\alpha$$

where $(N+1)\alpha = (n+1)\pi$. This modification has the effect of reducing the severity of the curvature change and the profile thus mapped is everywhere acceptably close to the given one.

2.2. Stress Potentials.

A large number of collocation points is used in calculating the stress potentials so as to reduce the chance of errors being introduced into the stress values. About 80 points are found to give satisfactory

results. If the number of points is increased unnecessarily the computing time increases whilst too small a number of points leaves the stress field lacking in the detail necessary for a satisfactory calculation.

Separate analyses are made for the uniaxial and for the shear loading cases. The various biaxial loadings are obtained by superposition of solutions obtained from the uniaxial case. The equations governing the stress potentials [equations (34) and (45) of Wittrick⁶] are linear in the coefficients of the stress functions but are non-linear in the mapping coefficients. This non-linearity arises from the variation of the reinforcement parameter Q with position. Because of this feature, it is unlikely that a procedure, more satisfactory than collocation, can be found for the numerical evaluation of the stress potentials.

2.3. Stress Criteria.

The results to be presented are given as variations of the Mises-Hencky criterion⁶ with structural parameters. In addition some results using the maximum principal stress criterion are shown and although there is some change in the value of the stress concentration using this second criterion, the variation with parameters is, qualitatively, much the same.

3. Discussion of Results.

The symbol $[f_1, f_2; q]$, as used in Ref. 3, describes the loading of the sheet far from the hole. f_1 and f_2 are tensions applied along the axes whilst q is an applied shear. Results are given for $[1, 0; 0]$, $[1, \frac{1}{2}; 0]$, $[1, 1; 0]$ and $[0, 0; 1]$ loadings. The results using the Mises-Hencky criterion are presented in Figs. 3 to 10 and using the maximum principal stress criterion in Figs. 11 to 18. Note that in the odd numbered diagrams, the abscissa is $\rho^{-\frac{1}{2}}$, where ρ is the ratio of quadrant radius to the semi-width of the hole (b). This representation emphasizes the essentially linear dependence of the stress envelope on $\rho^{-\frac{1}{2}}$.

It will be seen from the figures that for any given value of ρ , there is a value of the reinforcement parameter A' ($= A/bt$, A being area of cross section of the reinforcement and t the sheet thickness) which will minimise the stress concentration for a given loading. As ρ decreases, the optimum reinforcement decreases. That an optimum reinforcement exists for a given system follows from the fact that the introduction of a small amount of reinforcement restricts the edge strain, whilst too excessive a reinforcement leads to high normal and shear stresses occurring similar to the stresses at a completely restrained (built-in) corner.

For the truly quadrantal corner joined to straight sides of the hole, the normal stress induced into the sheet at the interface, under the chain reinforcement hypothesis, jumps at the point of curvature discontinuity. Thus it is possible, by ignoring the bending stiffness of the edge member to obtain a spurious result, since a real jump in normal stress on the edge of the sheet implies an infinite shear stress. Very high shear stresses arise only in the limiting case of negligible bending stiffness in the edge member. This detail is considered further in Appendix A.

A schematic representation of the Mises-Hencky stress variation is shown in Fig. 19 for a typical hole ($\rho = 0.5$) under uniaxial loading. This illustration shows how the presence of a small amount of reinforcement lowers the stresses as compared with an unreinforced case, and also shows how the stress accumulates in the corner when the reinforcement is excessive. Not only does the peak stress rise, but the region affected by high stress spreads throughout the quadrant. It is clear from this illustration that reinforcements in excess of the optimum are not only uneconomical in the weight of material used, but lead to an enlargement of the area of high stress.

The parameter η , which is defined as the weight of optimum reinforcement for a given system relative to the weight of sheet removed is plotted, as a function of ρ , in Figs. 20 to 23 for the four loadings discussed here. The parameter η has the value

$$\eta = \frac{2 \left[1 + \left(\frac{\pi}{4} - 1 \right) \rho \right] A'}{\left[1 + \left(\frac{\pi}{4} - 1 \right) \rho^2 \right]}$$

and in the range of ρ examined (0.2 to 1.0) lies between 1.93 A' and $2A'$. If the stress is allowed to rise to above the optimum a lighter reinforcement is possible and in Figs. 20 to 23, the values of η for stress excesses of 5, 10, 15 and 20 per cent are indicated. A reduction in weight, often of quite significant proportions, is achieved with a modest rise in stress. Thus it appears that striving for optimum reinforcement may be inadvisable.

The limiting profile, $\rho = 1.0$, is a circular one and this case can be analysed exactly. For all round tensile loading $[1, 1; 0]$ the hole is neutral for $A' = (1 - \nu)^{-1}$ or, for $\nu = 0.3$, $A' \approx 1.43$. For $\rho < 1$ the profiles are never neutral but, nevertheless, are often associated with low values of stress. The particular case of the circular hole is discussed in Appendix B. It should be noted that the reinforcement required to neutralise the hole is about 3 times the reinforcement required for optimum results in the uniaxial loading case.

Wittrick⁸ finds that the optimum profile of the 'rounded square' type has a stress concentration factor of 1.66 in $[1, \frac{1}{2}; 0]$ loading and that this compares unfavourably with the unreinforced elliptic hole, where the factor may be under 1.5. From Fig. 7 it will be seen that profiles which are nearly circular give stress concentrations of the order of 1.3 to 1.4 in biaxial loading. The discrepancy between Wittrick's results and those reported here lies in the difference in the profile. Wittrick's profiles do not include the circular element as a limiting case, that is, a profile with the right shape to be neutral. However his profiles, for $\rho < 0.5$, are adequate representations of the 'quadrantal corner'. For $0.5 < \rho$ the Wittrick results must be interpreted with care.

However, Wittrick's conclusion that the optimum performance with a hole of this type is inferior to an unreinforced elliptic hole, is endorsed, whilst a reinforced elliptic hole is a very good design indeed. The best that can be achieved with a rounded-square hole is a stress concentration factor in biaxial loading which is about 1.3 for a nearly circular hole: for the reinforced elliptic hole using reinforcement values markedly different from 'neutral hole' indications, the stress concentration factor can be kept down to the order of 1.1⁷.

Conclusion.

The computations made by Wittrick for a family of 'rounded-square' holes have been extended to the simulated 'quadrantal' corner. Stress concentrations for a wide variety of loadings are presented in graphical form for corner radii of 0.2 to 1 times the semi-width of the hole.

APPENDIX A

The Effect of a Finite Bending Stiffness of the Edge Reinforcement on the Shear Stress Under a Pressure Discontinuity (see para. 3)

In the main text, attention was drawn to the possibility of high stresses in the sheet at the reinforcement interface due to a pressure jump. This detail is analysed with the following model.

Given an elastic strip of thickness t occupying the region bounded by $y = \pm a$ which has an edge member on $y = \pm a$ of constant cross-sectional area B and bending stiffness EI . Suppose the system is acted upon by a pressure loading $p(x)$ which is an odd function of x and $p(x)$ does not tend to zero as $x \rightarrow 0$ from either side. Such a model is a valid representation of the local conditions under a curvature discontinuity. Since we are seeking a local effect, the boundary can be assumed straightened and a discontinuous load introduced to simulate the curvature jump.

We seek an Airy stress function ϕ for the sheet satisfying $\nabla^4 \phi = 0$ in the sheet together with boundary conditions

$$\frac{\partial}{\partial x} \left(\frac{\partial^2 \phi}{\partial y^2} - \nu \frac{\partial^2 \phi}{\partial x^2} \right) = -\frac{t}{B} \frac{\partial^2 \phi}{\partial x \partial y}$$

and

$$EI \frac{\partial^4 v}{\partial x^4} + t \frac{\partial^2 \varphi}{\partial x^2} = -p(x) \quad \text{on } y = \pm a$$

where

$$Ev = \int_0^a \frac{\partial^2 \varphi}{\partial x^2} dy - v \left[\frac{\partial \varphi}{\partial y} \right]_{y=a}$$

The general solution of $\nabla^4 \varphi = 0$ of the form $\varphi = \sin \lambda x F(y)$, where $F(y)$ is even in y is

$$\varphi(x, y) = \int_0^\infty [A_1(\lambda) \cosh \lambda y + A_2(\lambda) \lambda y \sinh \lambda y] \sin \lambda x d\lambda.$$

The first boundary condition gives

$$A_1 U_1 + A_2 U_2 = 0$$

where $U_1 = Q(1 + \nu) \theta \cosh \theta + \sinh \theta$

$$U_2 = Q(1 + \nu) \theta^2 \sinh \theta + (2Q + 1) \theta \cosh \theta + \sinh \theta$$

$$Q = B/at$$

and $\theta = a\lambda$.

The second boundary condition gives

$$\lambda^2 (V_1 A_1 + V_2 A_2) = \frac{2}{\pi} \int_0^\infty P(x) \sin \lambda x dx = \bar{p}(\lambda) \text{ say}$$

where $V_1 = \left(\frac{I}{a^3}\right) (1 + \nu) \theta^3 \sinh \theta + t \cosh \theta$

and $V_2 = -\left(\frac{I}{a^3}\right) (1 - \nu) \theta^3 \sinh \theta + \left(\frac{I}{a^3}\right) (1 + \nu) \theta^4 \cosh \theta + t \theta \sinh \theta$

so that

$$\lambda^2 A_1 = \frac{U_2 \bar{p}(\lambda)}{V_1 U_2 - V_2 U_1} \quad \text{and} \quad \lambda^2 A_2 = \frac{-\bar{p}(\lambda) U_1}{V_1 U_2 - V_2 U_1}.$$

The required shear stress is $-\frac{\partial^2 \varphi}{\partial x \partial y}$ evaluated for $x = 0, y = a$ and has the value $-\int_0^\infty \lambda^2 [(A_1 + A_2)]$

$\sinh \theta + A_2 \theta \cosh \theta] d\lambda$. On substituting for $A_1(\lambda)$ and $A_2(\lambda)$ this has the value

$$\int_0^{\infty} \frac{Q [(1+\nu) \theta^2 - (1-\nu) \theta \cosh \theta \sinh \theta] \bar{p}(\theta) d\theta}{\frac{I}{a^3} F_1(\theta) + t F_2(\theta)}$$

where $F_1(\theta) = -(1+\nu)^2 Q \theta^5 + (1+\nu)(3-\nu) Q \theta^4 \cosh \theta \sinh \theta + 2\theta^3 \sinh^2 \theta$

and $F_2(\theta) = 2Q \theta \cosh^2 \theta + \cosh \theta \sinh \theta + \theta$.

A convenient function for $p(x)$ is to take $p(x) = p$ for $x \leq b$ and zero for $x > b$ so that

$$\bar{p}(\theta) = -\frac{4ap}{\pi\theta} \sin^2 \left(\frac{b\theta}{2a} \right).$$

In a practical example, it is convenient to take $a = 20$, $b = 20$, $t = 0.1$, $B = 0.5$, $I = 0.05$, so that $p = 0.025T$, where T is the tension in the reinforcement at the junction.

The integral is evaluated numerically and has the value $0.246T$. This example illustrates the absence of a significant stress concentration in a practical system.

APPENDIX B

Circular Reinforced Holes (see para. 3)

If a sheet containing a reinforced, circular hole is subjected to axial tensions f_1, f_2 say, the stresses around the sheet are (from Ref. 5, equation (34)) given as

$$\sigma_n = \frac{Q}{2} \left(f_1 + f_2 - \frac{2}{1+Q} (f_1 - f_2) \cos 2\theta \right)$$

$$\sigma_s = \left(1 - \frac{Q}{2} \right) \left(f_1 + f_2 - \frac{2}{1+Q} (f_1 - f_2) \cos 2\theta \right)$$

and

$$\tau = \frac{2Q}{1+Q} (f_1 - f_2) \sin 2\theta.$$

Q is the reinforcement parameter $\frac{2A'}{(1+\nu)A'+1}$.

For shear loads S acting alone the corresponding stresses are (Ref. 5, equation (45)) given as

$$\sigma_n = -\frac{2QS}{1+Q} \sin 2\theta$$

$$\sigma_s = \frac{2(Q-2)S}{1+Q} \sin 2\theta$$

and

$$\tau = -\frac{4QS}{1+Q} \cos 2\theta.$$

For the 4 basic loadings considered in the text, the minimum possible Mises-Hencky stresses and associated reinforcement parameter A' are (for $\nu = 0.3$) as under:

Loading	[1, 0; 0]	[1, $\frac{1}{2}$; 0]	[1, 1; 0]	[0, 0; 1]
Minimum Mises-Hencky stress	1.493	1.325	1.0	1.167
A' for min stress (A'_{opt})	0.445	0.984	1.429	0.281
Relative stress at $A' = 0.5A'_{opt}$	126%	113%	110%	133%

From this Table it is clear that optimum reinforcement requires the use of an unnecessarily heavy member. By reducing the reinforcement weight by half, the penalty in stress is small and the weight saved may be used advantageously elsewhere in the structure. In all round tension the optimum reinforcement neutralises the hole and leads to a very heavy design ($A' \approx 1.4$) with a reinforcement weight of about three times the weight of sheet removed.

The behaviour of nearly circular holes (i.e. $\rho \approx 0.7$) is broadly similar.

LIST OF SYMBOLS

A	Area of cross-section of reinforcement
A'	Reinforcement parameter ($= A/bt$)
b	Semi-width of hole
C_n	Real coefficients in the mapping function which relates z and ζ
F	Mises-Hencky stress
f_1, f_2, q	Direct stresses and shear stress which are applied to the sheet at a great distance from the hole
N	Terminating index in polynomial representation of z
Q	Reinforcement parameter ($= 2A'\{(1+\nu)A'+1\}^{-1}$)
s, n	Tangential and normal co-ordinates on the boundary of the hole
t	Thickness of the sheet
x, y	Cartesian co-ordinates in the plane of the sheet
z	Complex variable ($= x + iy$)
ζ	An auxiliary complex variable
η	Reinforcement weight divided by weight of sheet removed to form the hole
θ	Argument of ζ
ν	Poisson's ratio (taken to be 0.3)
ρ	b^{-1} times radius of corner quadrant
σ_n, σ_t, τ	Direct stresses and shear stress referred to the s, n axes at a point on the boundary of the hole

REFERENCES

- | No. | Author(s) | Title, etc. |
|-----|----------------------------|---|
| 1 | N. I. Muskhelishvili | <i>Some basic problems of the mathematical theory of elasticity.</i>
Noordhoff, Groningen, 1953. |
| 2 | A. J. Sobey | The estimation of stresses around unreinforced holes in infinite elastic sheets.
A.R.C. R. & M. 3354, October 1962. |
| 3 | A. J. Sobey | Stress-concentration factors for rounded rectangular holes in infinite sheets.
A.R.C. R. & M. 3407, November 1963. |
| 4 | E. H. Mansfield | Neutral holes in plane sheet—reinforced holes which are elastically equivalent to the uncut sheet.
<i>QJMAM</i> , VI, 3, 370, 1953. |
| 5 | E. H. Mansfield | Stress considerations in the design of pressurised shells.
A.R.C. C.P. 217, April 1955. |
| 6 | W. H. Wittrick | Analysis of stress concentrations at reinforced holes in infinite sheets.
<i>Aero. Quart.</i> XI, pp. 233–247, 1960. |
| 7 | W. H. Wittrick | Stresses around reinforced elliptic holes with applications to pressure cabin windows.
<i>Aero. Quart.</i> X, pp. 373–400, 1959. |
| 8 | W. H. Wittrick | Stress concentrations for a family of uniformly reinforced square holes with rounded corners.
<i>Aero. Quart.</i> XIII, pp. 223–234, 1962. |
| 9 | Cornelius Lanczos | <i>Linear differential operators</i> , paras. 2.9, 2.14.
Van Nostrand, 1961. |

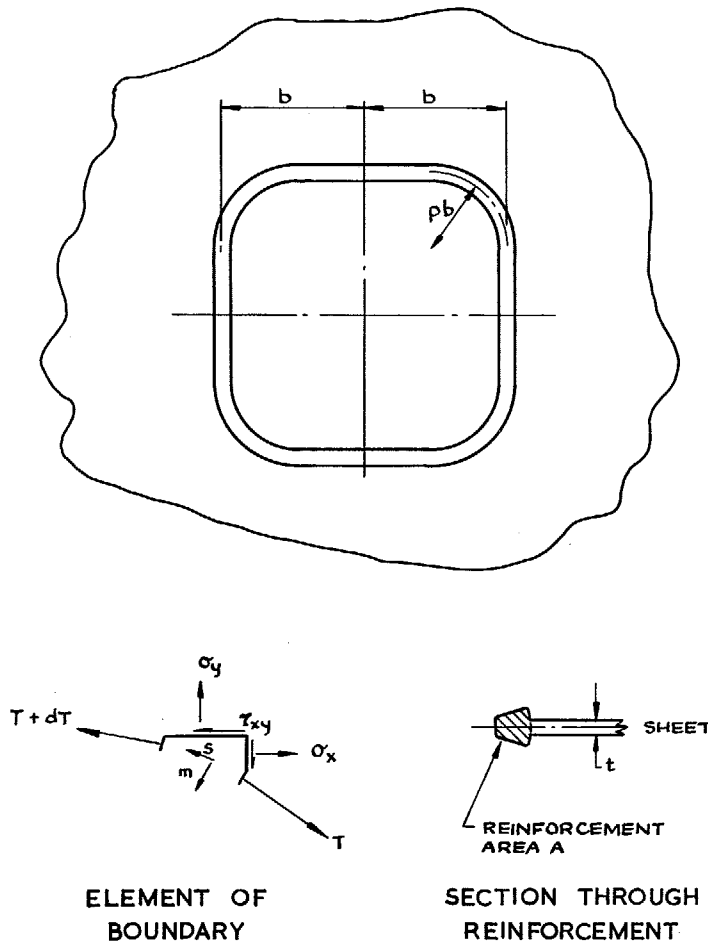


FIG. 1. Profile of reinforced hole with element.

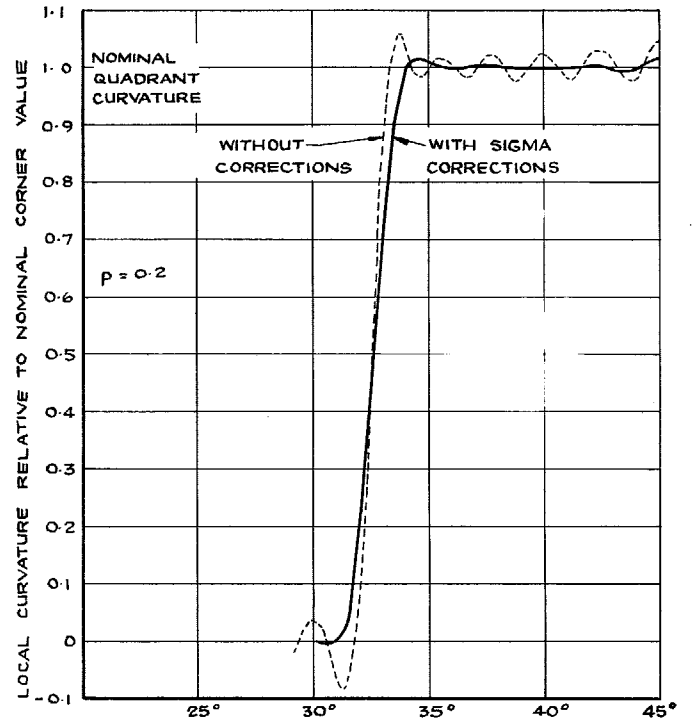


FIG. 2. Profile smoothing by Sigma correction.

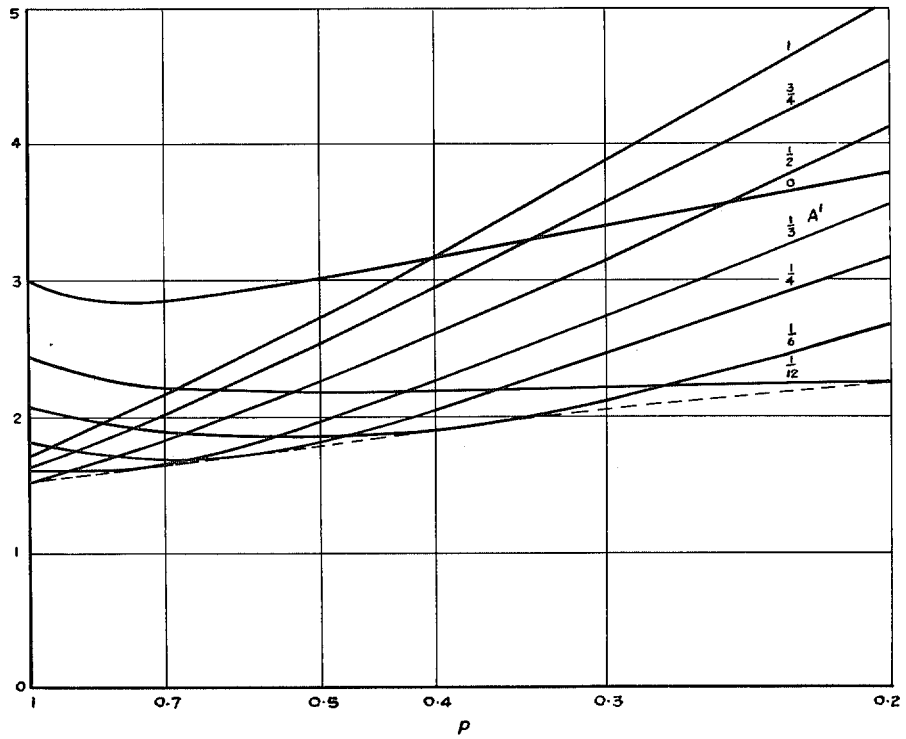


FIG. 3. Mises-Hencky stress as a function of A' and ρ for $[1, 0; 0]$ loading.

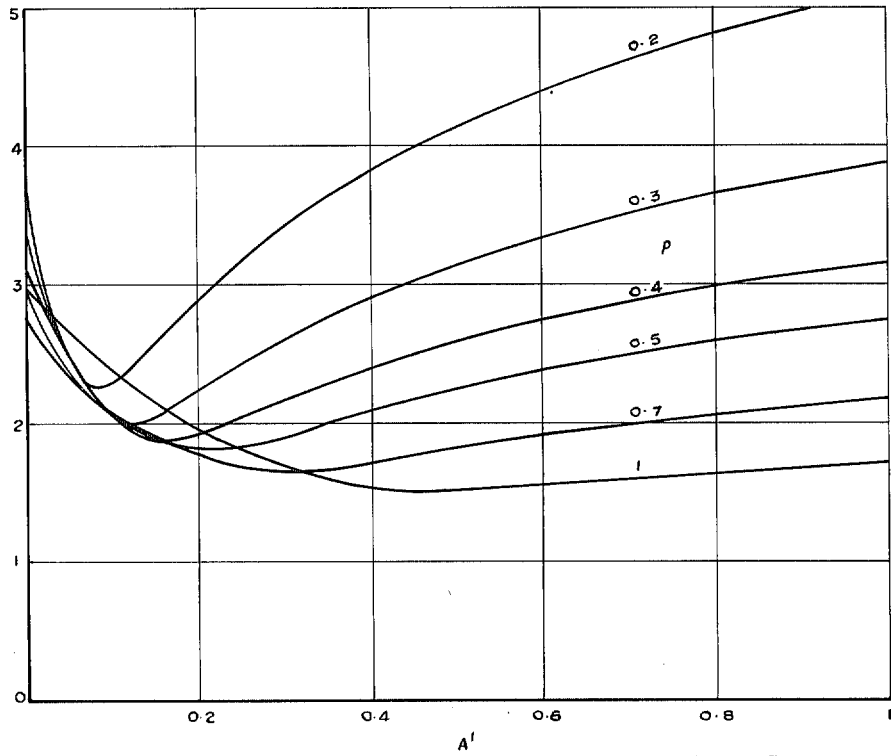


FIG. 4. Mises-Hencky stress as a function of ρ and A' for $[1, 0; 0]$ loading.

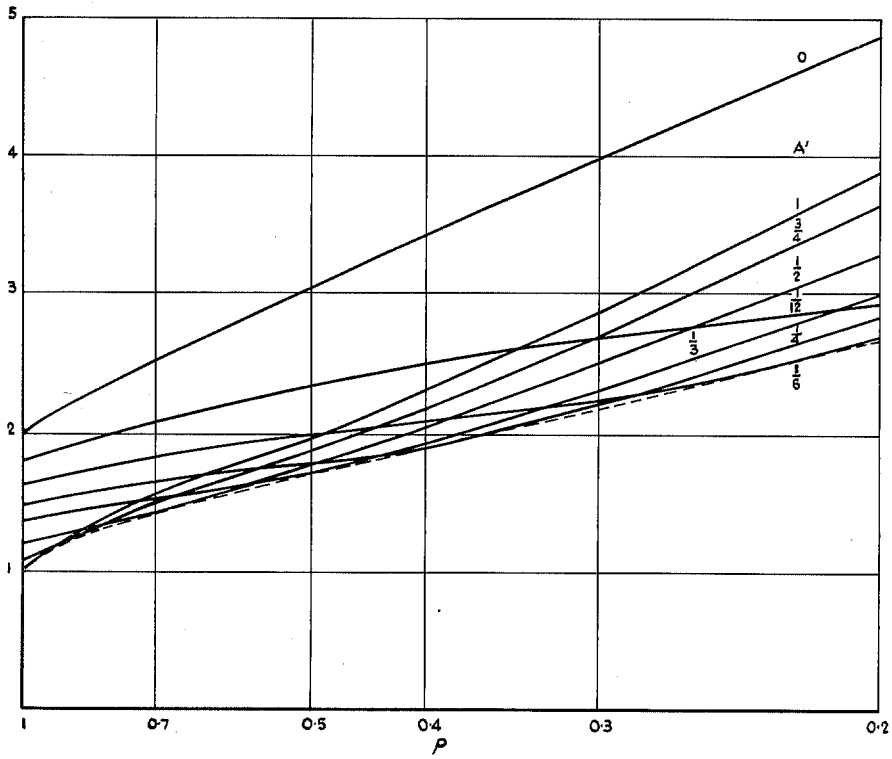


FIG. 5. Mises-Hencky stress as a function of A' and ρ for $[1, 1; 0]$ loading.

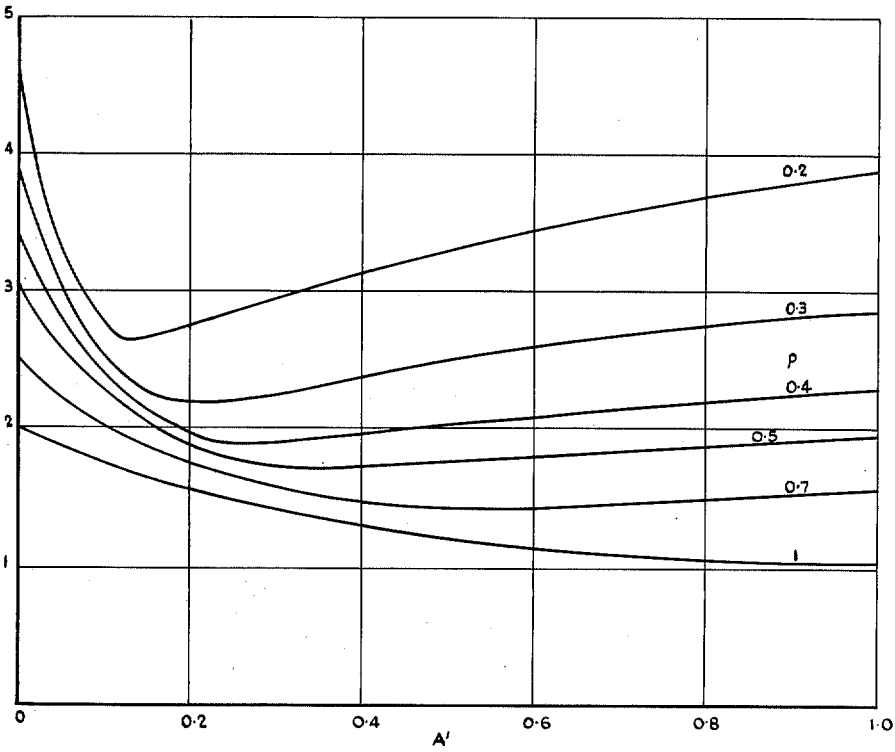


FIG. 6. Mises-Hencky stress as a function of ρ and A' for $[1, 1; 0]$ loading.

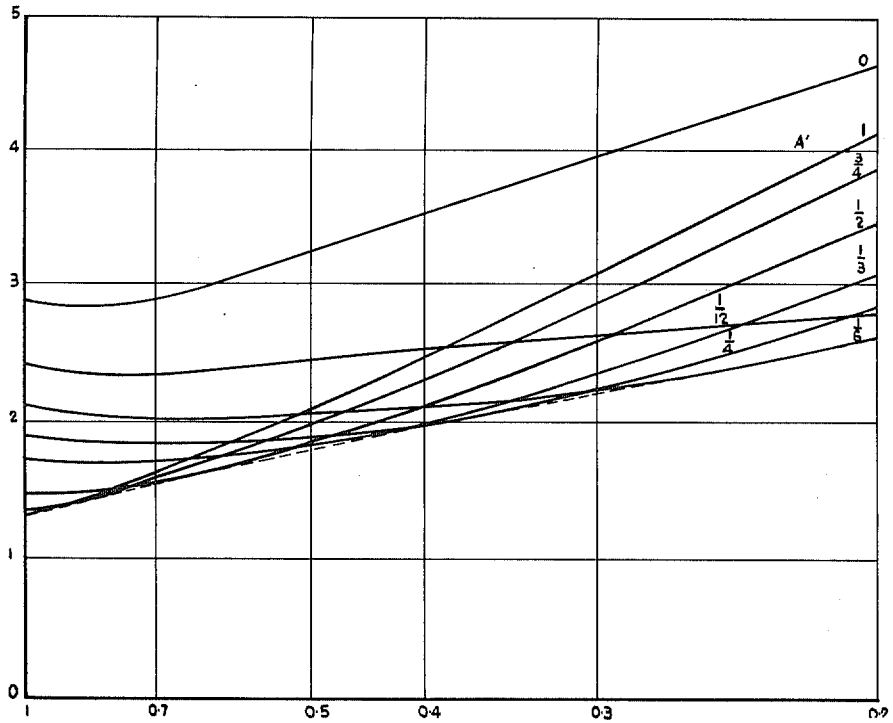


FIG. 7. Mises-Hencky stress as a function of A' and ρ for $[2, 1; 0]$ loading.

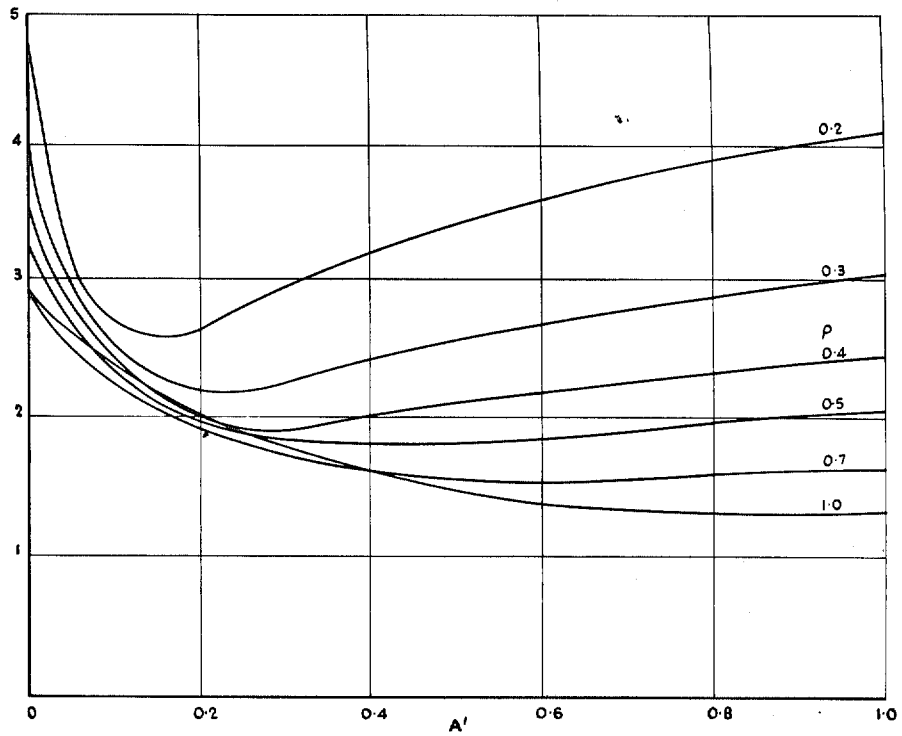


FIG. 8. Mises-Hencky stress as a function of ρ and A' for $[2, 1; 0]$ loading.

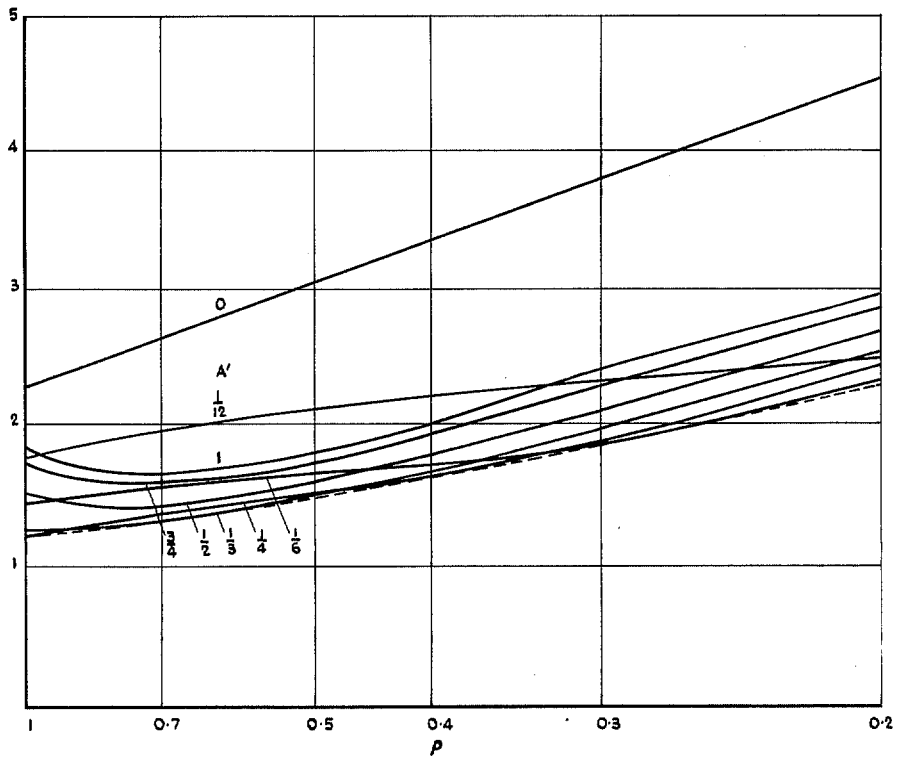


FIG. 9. Mises-Hencky stress as a function of A' and ρ for $[0, 0; 1]$ loading.

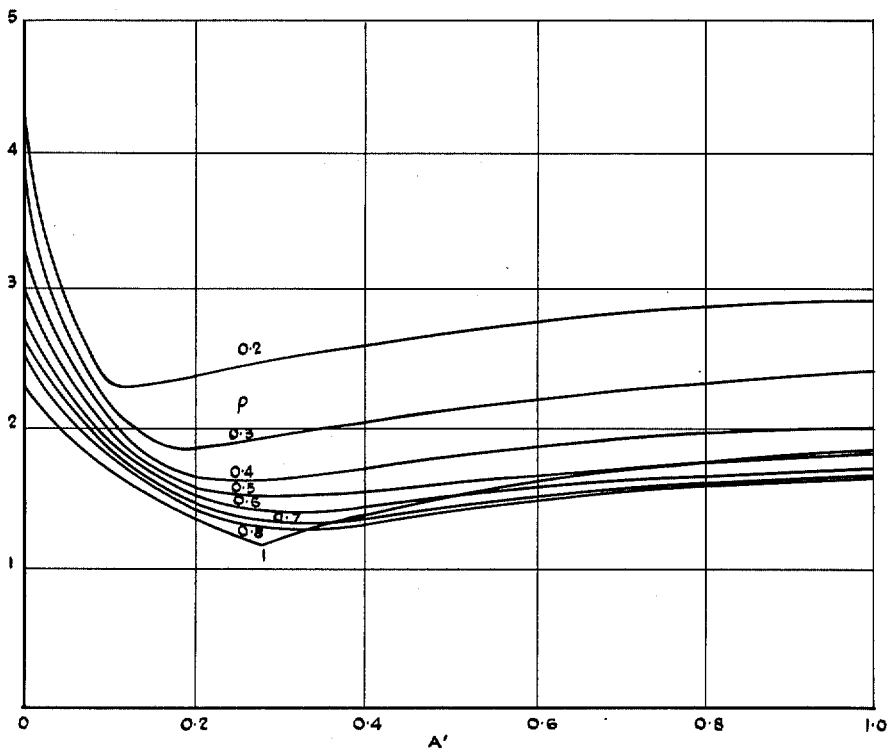


FIG. 10. Mises-Hencky stress as a function of ρ and A' for $[0, 0; 1]$ loading.

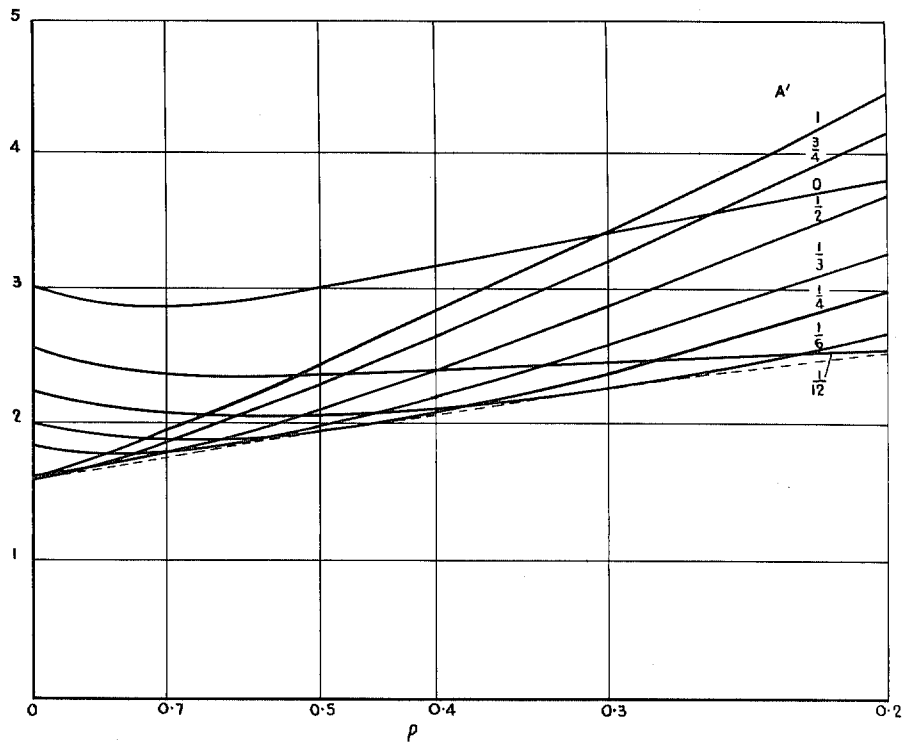


FIG. 11. Maximum principal stress as a function of A' and ρ for $[1, 0; 0]$ loading.

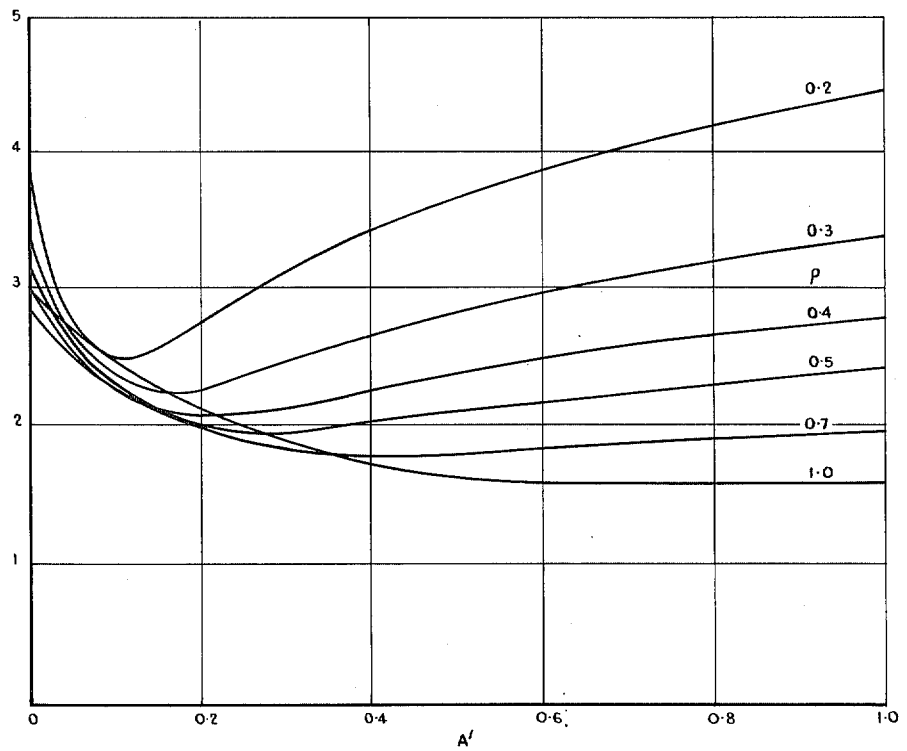


FIG. 12. Maximum principal stress as a function of ρ and A' for $[1, 0; 0]$ loading.

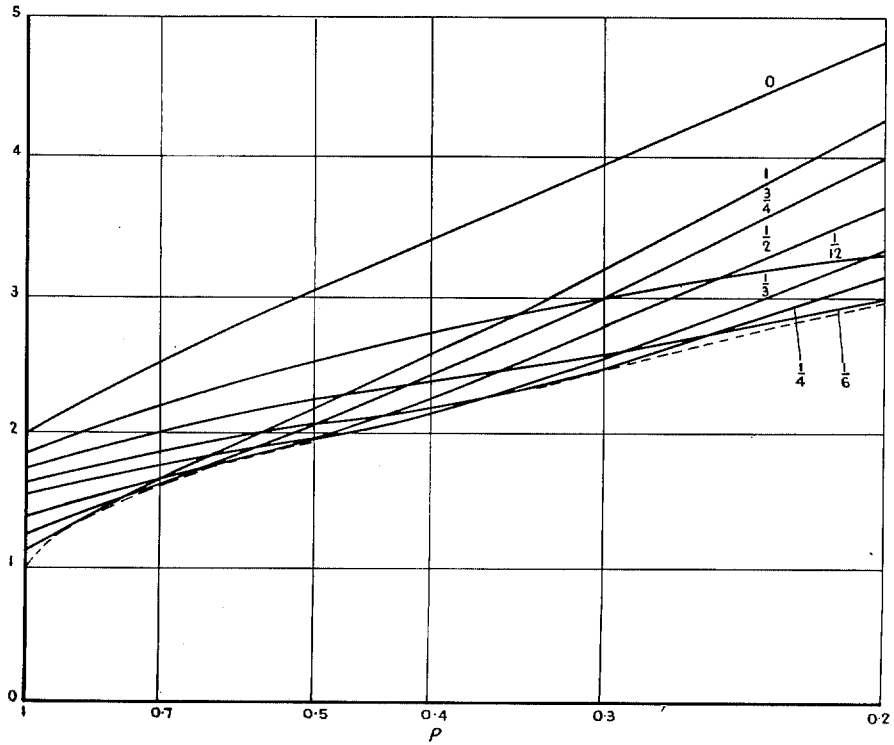


FIG. 13. Maximum principal stress as a function of A' and ρ for $[1, 1; 0]$ loading.

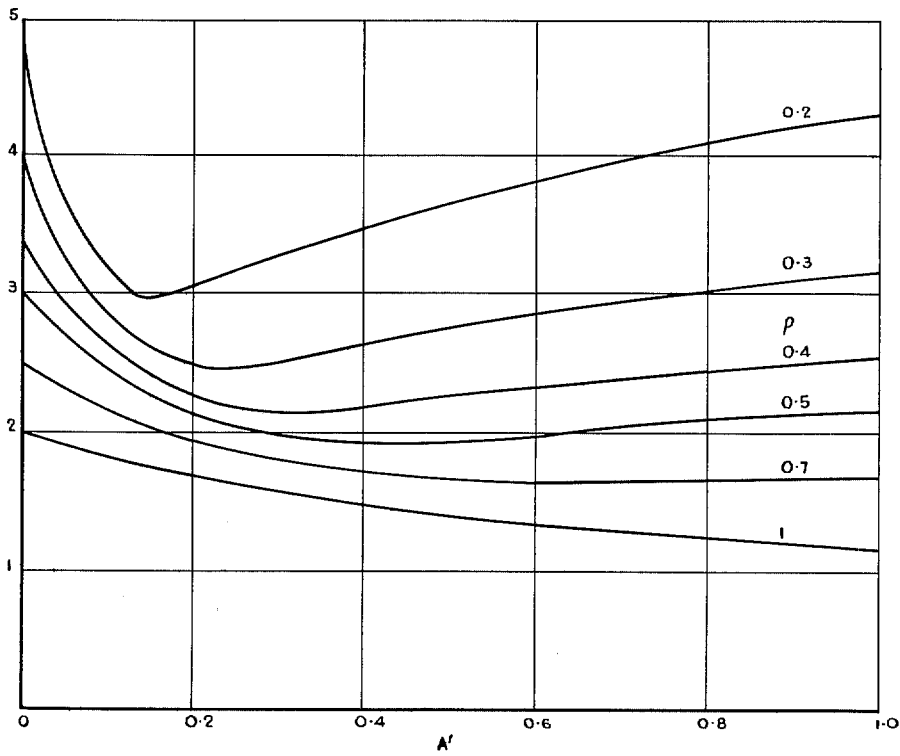


FIG. 14. Maximum principal stress as a function of ρ and A' for $[1, 1; 0]$ loading.

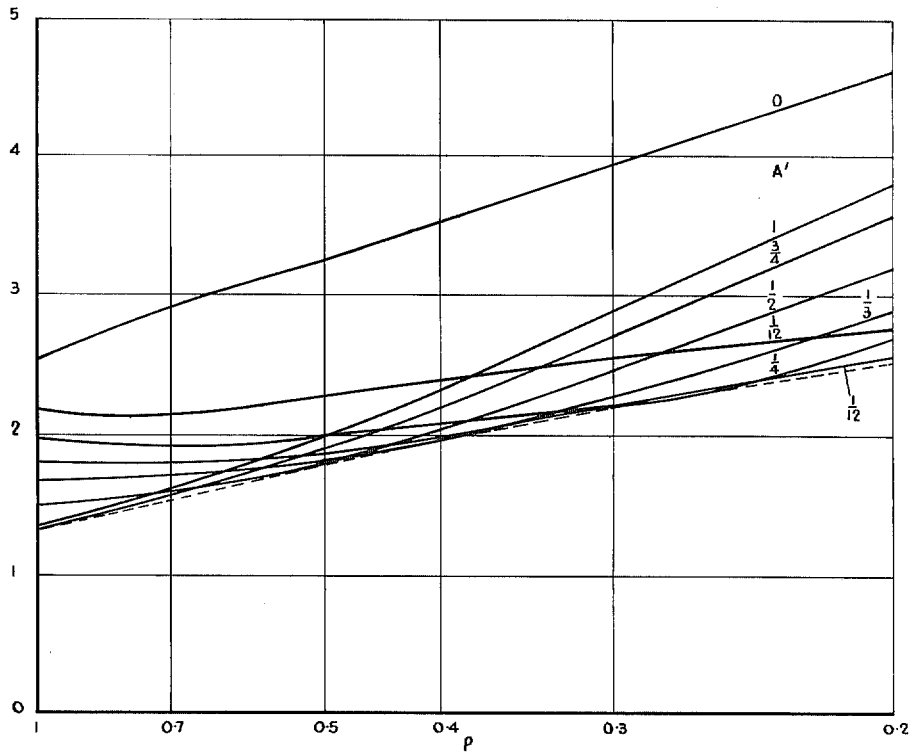


FIG. 15. Maximum principal stress as a function of A' and ρ for [2, 1; 0] loading.

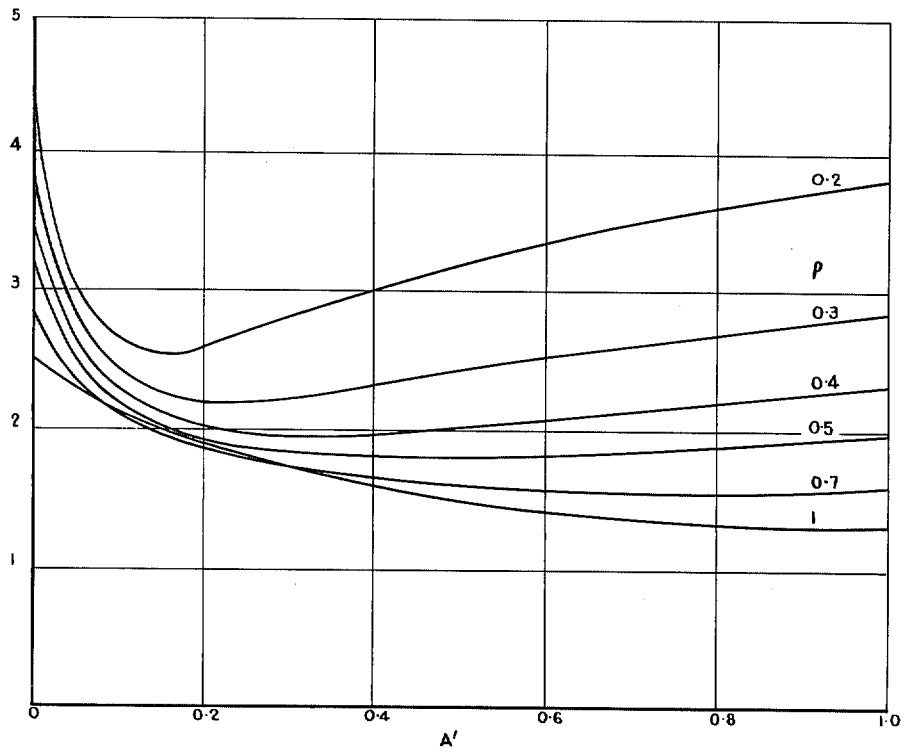


FIG. 16. Maximum principal stress as a function of ρ and A' for [2, 1; 0] loading.

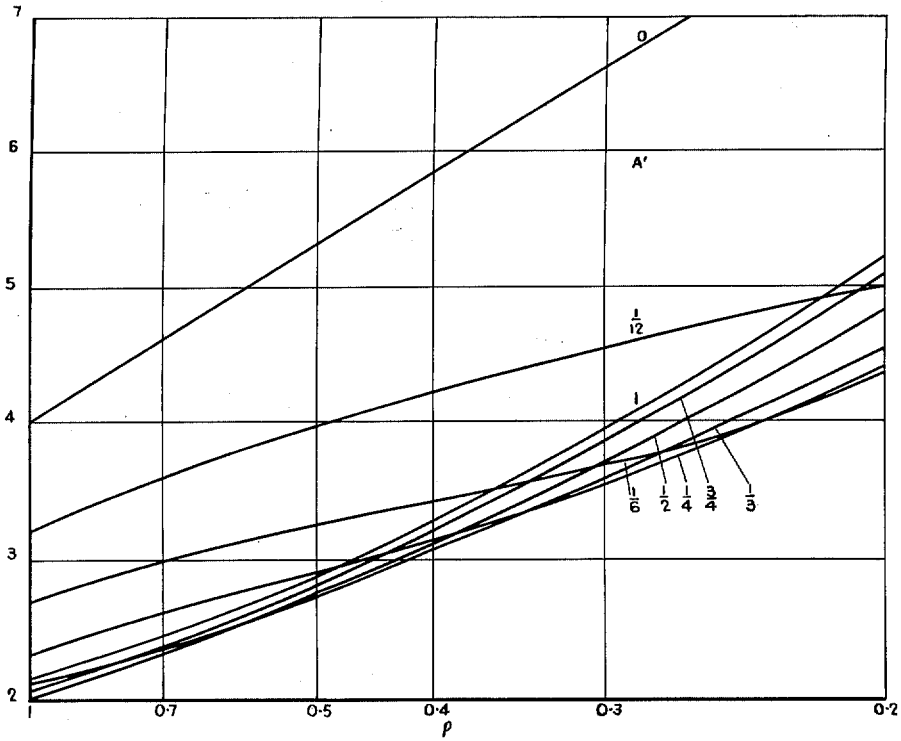


FIG. 17. Maximum principal stress as a function of A' and ρ for $[0, 0; 1]$ loading.

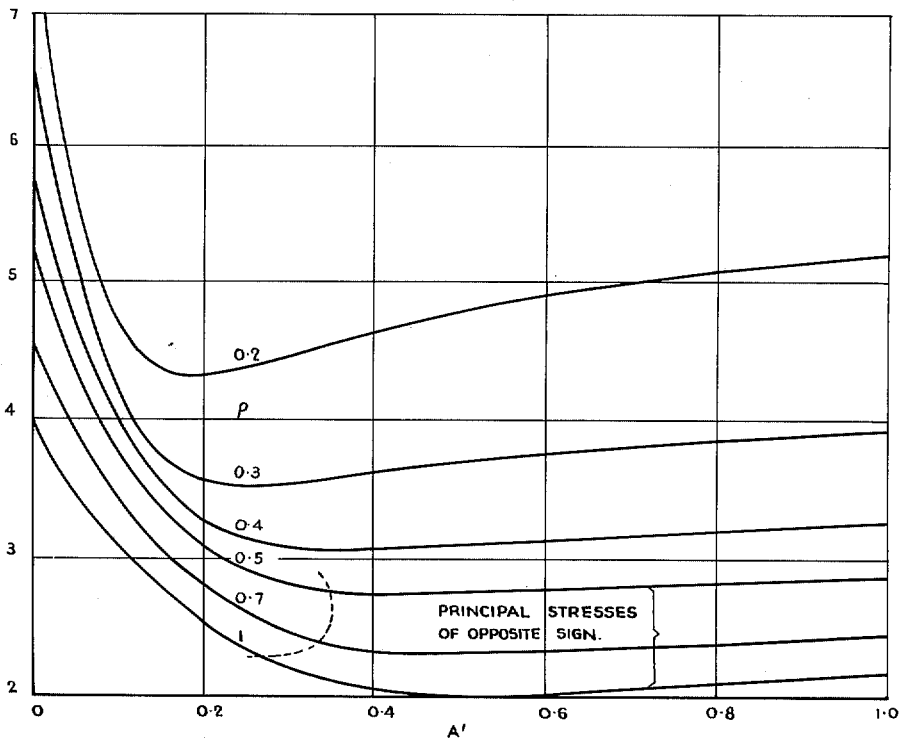


FIG. 18. Maximum principal stress as a function of ρ and A' for $[0, 0; 1]$ loading.

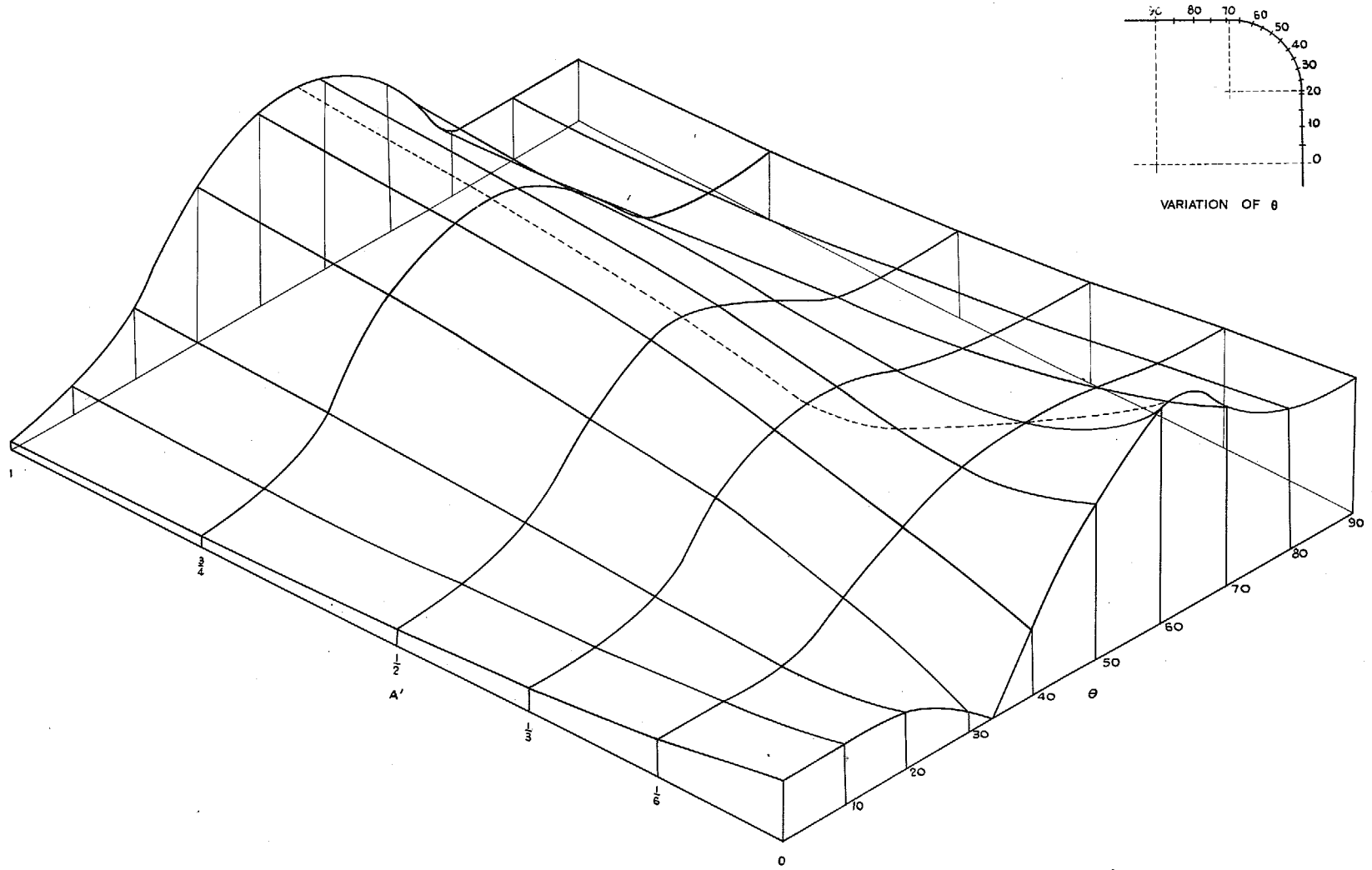


FIG. 19. Mises-Hencky stress variation around quadrant as a function of A' for $\rho = 0.5$ in. uniaxial

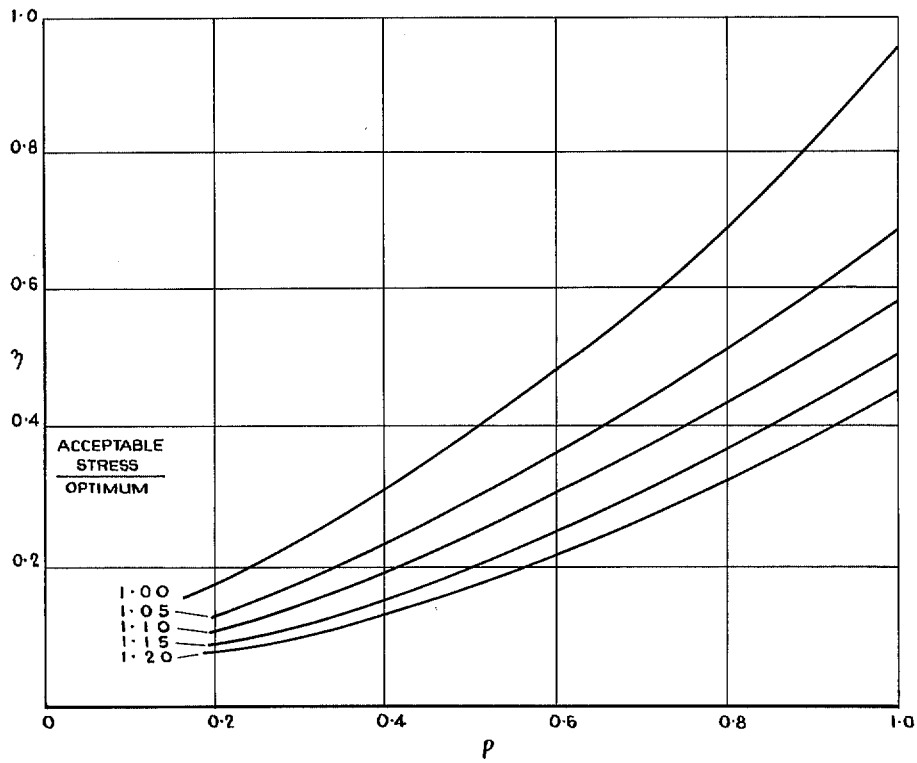


FIG. 20. Variation of reinforcement weight with ρ in optimum (and other) reinforcement, [1,0;0] loading.

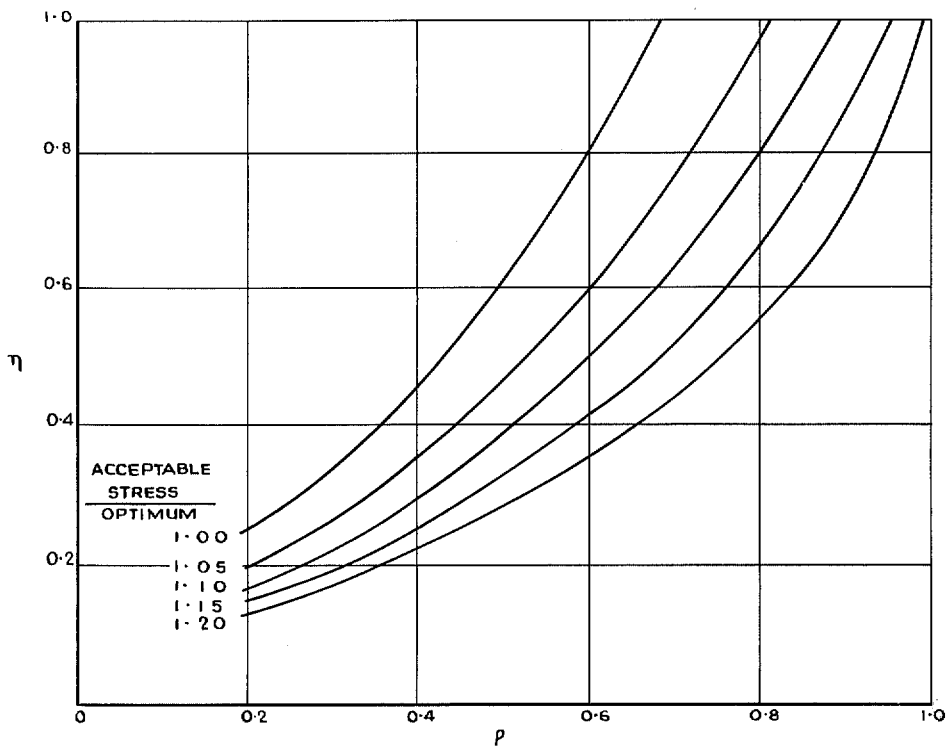


FIG. 21. Variation of reinforcement weight with ρ in optimum (and other) reinforcement [1,1;0] loading.

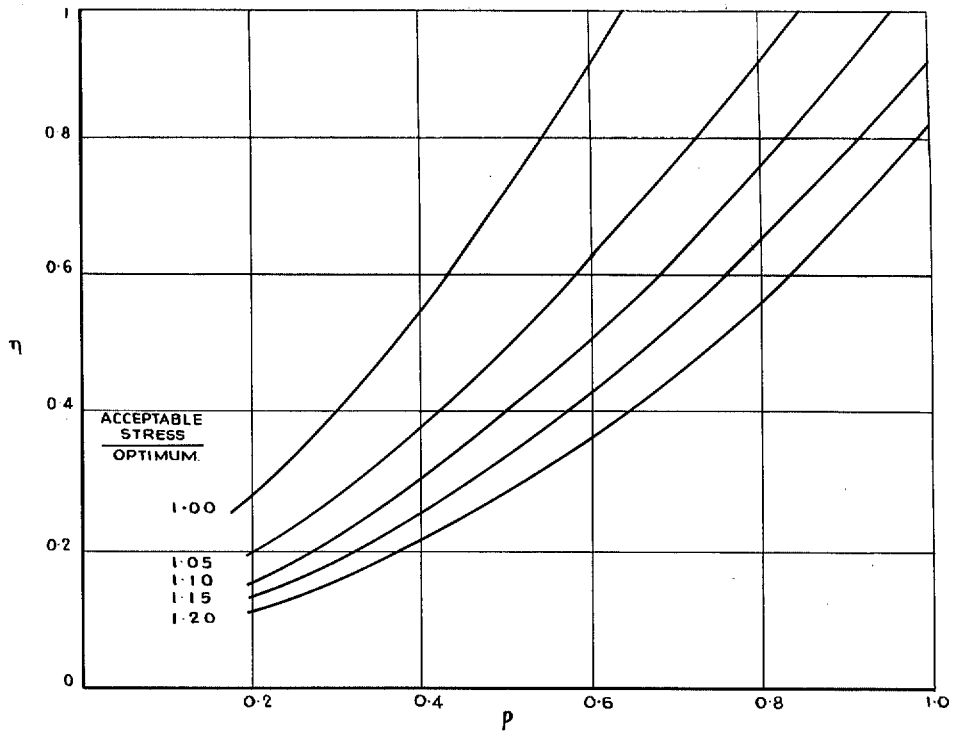


FIG. 22. Variation of reinforcement weight with ρ in optimum (and other) reinforcement $[2, 1; 0]$ loading.

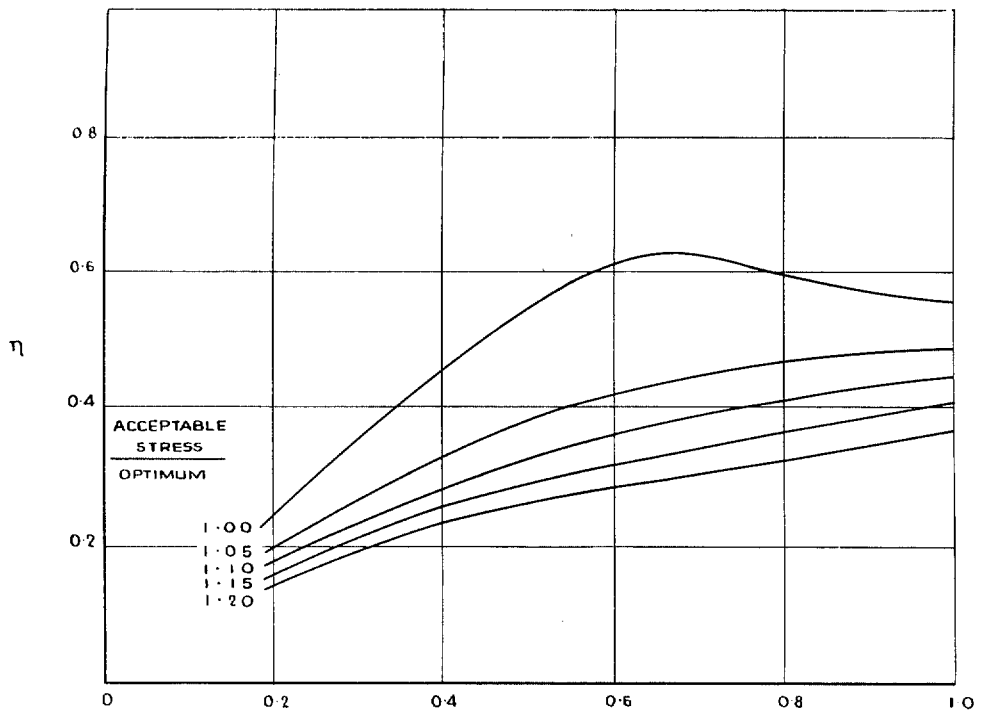


FIG. 23. Variation of reinforcement weight with ρ in optimum (and other) reinforcement $[0, 0; 1]$ loading.

© Crown copyright 1968

Published by
HER MAJESTY'S STATIONERY OFFICE

To be purchased from
49 High Holborn, London W.C.1
423 Oxford Street, London W.1
13A Castle Street, Edinburgh 2
109 St. Mary Street, Cardiff CF1 1JW
Brazenose Street, Manchester 2
50 Fairfax Street, Bristol 1
258-259 Broad Street, Birmingham 1
7-11 Linenhall Street, Belfast BT2 8AY
or through any bookseller